Al-Rafidain Journal of Engineering Sciences

Journal homepage https://rjes.iq/index.php/rjes

ISSN 3005-3153 (Online)

Experimental and Numerical Enhancement of Solar PV Panel Performance Using Anti-Reflective Coatings and MPPT Control Algorithms

Falah Hassan Mohammed

Assistant Governor for planning Affairs, Wasit, Iraq

ARTICLE INFO

Article history:

Received	22 December 2025
Revised	22 December 2025
Accepted	20 January 2026
Available online	21 January 2026

Keywords:

Photovoltaic (PV) systems
SiO_2 anti-reflective coating
Maximum power point tracking (MPPT)
Fuzzy logic control

ABSTRACT

In this review we describe the experimental and numerical research about improving the performance of a PV system using the combined application of a SiO_2 anti-reflective (AR) coating and an advanced maximum power point tracking (MPPT) algorithm to achieve improvements. Through the combination of a DC–DC converter and a parallel lithium-ion battery pack, a microscale PV prototype was developed and tested for steady-state and dynamic irradiance conditions. The initial PV voltage increased from 3.45 V to 3.50 V and the current from 1.30 A to 1.45 A from the SiO_2 coating, in this, an increase of 4.6 W to 5.1 W is noticed, which relates to an enhancement of 10–12% power output, respectively. At 60 min, the coated panel kept a higher power (≈1.35 W) and efficiency (≈29%) than the baseline panel (1.25 W and ≈26%). The performance of four modes—no MPPT, Perturb and Observe (P&O), Incremental Conductance (INC) and Fuzzy Logic MPPT—was investigated. Fuzzy Logic MPPT produced the greatest power output (4.45 W in the beginning and ≈1.4 W after 60 minutes), with the best tracking efficiency of about 95%, better than P&O (≈85%) / INC (≈91%) respectively. The fuzzy logic controller remained close to theoretical peak at rapid irradiances of 800 to 500 W/m² (≈5.1 W and ≈3.2 W) with low tracking error (2–3%) and fastest convergence time of ≈9 s. The harvested power maximum was reached around 0.91 Wh with SiO_2 coated and fuzzy logic MPPT, while 0.67 Wh was reached for the baseline system without MPPT. Analysis of the battery charging indicated higher state of charge from 21% to 56–57%, and the total energy delivered to the battery increased from 2.0 Wh to 2.7 Wh. The findings are suggestive of the efficiency of the integration of the surface design and intelligent MPPT control, that enhance the output electricity of photovoltaic (PV) systems, energy harvesting, dynamic response and battery charging performance, giving effective and scalable system for PV-based high-efficiency renewable energy system.

1. Introduction

As the world continues to push hard for cleaner and sustainable energy, photovoltaics (PV) have emerged as among the most attractive solar-based clean energy technologies due to their broad scaling, environmental compatibility and the lower installed cost. Despite these merits, PV modules' electrical performance is still significantly influenced by optical losses, temperature, and poor operating conditions, which restrict the energy conversion efficiency. Light loss due to surface reflection is generally enough to explain a significant portion of incident solar radiation, whereas rapid temperature and irradiance change leads PV modules to be operated away from their maximum power point, which is associated with a limited energy extraction and energy production. Anti-reflective (AR) coatings have

Corresponding author E-mail address: falah.hassanm1976@gmail.com
https://doi.org/10.61268/maaesr09

been extensively investigated in terms of surface engineering to reduce optical losses. Silicon dioxide (SiO_2) has received significant attention from different materials owing to its low refractive index, high optical transparency, chemical stability and compatibility with PV module surfaces. SiO_2-based coatings inhibit surface reflection and promote light entry into the active semiconductor layer, which ultimately increases the density of photogenerated carriers and enhances electrical output. Recent findings established that appropriately constructed AR coatings can lead to significant improvements in PV voltage, current and power production, especially in low- to moderate-irradiance conditions. Concurrent with the physical enhancements, maximum power point tracking (MPPT) approaches are fundamental in the performance of the electrical system of PV systems. The conventional MPPT methods, e.g., Perturb and Observe (P&O) and Incremental Conductance (INC), are commonly used as they are straightforward and easy to follow. But these techniques tend to remain prone to steady-state oscillations, slow convergence and low tracking accuracy in fast environmental change. To address these limitations, intelligent control solutions which depend on fuzzy logic-based MPPT have been suggested as viable alternatives for dealing with system nonlinearities and uncertainties, without having an exact mathematical model. Whilst there have been many papers specifically on AR coatings and MPPT algorithms in isolation, few studies have tested the effect of combined surface engineering and intelligent MPPT control on short-term power output and long-term energy harvesting performance. Furthermore, many studies mainly focus on steady-state behavior, but there has been a lack of analysis on the dynamic performance metrics (tracking error, convergence time, harvested energy, and battery charging efficiency). Especially when small-scale PV systems, intended for practical purposes like portable power or distributed energy applications, are concerned.

(Afonso et al., 2025) [1] systematically study the environmental effects on degradation and performance of PV materials over the long-term or short-term of both solar radiation and temperature exposure. It presents aging mechanisms and emphasizes the need for climate-adaptive PV material design. (Artuk et al., 2024) [2] The ALD-deposited Al_2O_3 interlayer enhances perovskite/C60 interfaces, thus improving the stability and energy efficiency. This study has already showcased promising perovskite–silicon tandem solar cell development. (Badran & Dhimish, 2023) [3] present potential induced degradation (PID) of PV modules. These findings are summarized and its mechanisms, detection methods and ways to prevent PV-induced degradation are discussed. It highlights the significance of system grounding and material optimisation. (Baradieh et al., 2024) [4] investigated how PV model parameters, DC-side faults affect the performance and I–V of an array. The study will provide guidance on faults diagnosis for a more accurate PV system modeling. (Brahim et al., 2024) [5] presents a dynamic Simulink/MATLAB model of a roll-bond PVT collector that is used with thermal-electrical relationship studies. Dynamic simulation proved useful in predicting the transient PVT behavior. (Calcabrini et al., 2022) [6] promote solar cells with relatively low-breakdown-voltage to provide higher shading resistance in PV modules and solar cells for reducing the PV module shading failure. The strategy effectively decreases power losses under partial shading. (Datta et al., 2023) [7] extensive review presents machine learning applications of PV manufacturing, monitoring and performance prediction. It emphasizes the contribution of ML in optimising production, fault detection and system planning and use. (Diniță et al., 2025) [8] introduces an IoT driven predictive maintenance approach via cloud ML for solar panels. The results show greater accuracy of fault prediction and lower cost of maintenance in the Industry 4.0 environment. (Elnozahy et al., 2024) [9] Hydrophilic nano-material coatings will help in better PV energy harvesting for eco-buildings, according to the research. Results showed better thermal regulation and electrical output. (Iturralde Carrera, Alfonso-Francia, et al., 2025) [10] systematic review reviews recent development trends of optimization for PV systems, such as AI-powered control and power electronics. It identifies optimization gaps in

hybrid and smart PV technology. (Iturralde Carrera, Garcia-Barajas, et al., 2025) [11] contribution sets out the significant factors that will impact PV efficiency and sustainability according to the materials, system design and environmental impacts. Long-term sustainability by new technologies is highlighted. (Jacob & Farzaneh, 2025) [12] employs dynamic simulation and optimization design to model a combination PV-wind-battery microgrid. Performance results indicate that in varying conditions, greater reliability and energy management can be demonstrated. (Lazaroiu et al., 2023) [13] explores PV technologies at large, so they can contribute to achieving climate neutrality. It contrasts traditional with emerging PV technologies from a sustainability perspective. (Liu et al., 2025) [14] present a front-side optical–thermal coupling strategy for simultaneous solar water heating and electricity generation in the study. Improved co-generation efficiency is reported with notable gains. (Liu et al., 2024) [15] present a real-time, computer-vision-based shadow detection system for the PV modules. The proposed method makes shading detection closer to reality, which makes operational reliability soar. (Mamodiya et al., 2025) [16] AI, smart materials, and adaptive PV in hybrid solar are integrated for study of hybrid solar system. Findings indicated a better adaptability and sustainable development of power. (Muthuvel Raj & Pawan Kumar, 2024) [17] assesses contemporary PV power system processes and their effects on efficiency and grid connections. Modern control and power management is emphasized. (Oproescu et al., 2024) [18] The effect of supplementary oxide layers on the solar cell is the topic of this study. Surface and interface engineering is demonstrated to have enhanced electrical properties. (Oulefki et al., 2024) [19] unsupervised sensing framework coupled with 3D augmented reality is proposed for the detection of degraded PV areas. The approach improves both visualization and maintenance decision making. (Rajendran et al., 2025) [20] integration of PV with smart grid is focused in this review, with a view to solutions, standards and grid codes. It underlines the importance of harmonized regulations and sophisticated control measures. (Ramasamy et al., 2023) [21] optimize PTFE-modified silica hydrosol coatings based on ANN and RSM. These coatings dramatically improve PV performance, with significant results in the reduction of thermal and optical losses. (Sadiq & Garba Ibrahim, 2025) [22] provides an overview of recent PV developments, the key challenges in implementing new technologies, and future prospects. Policy, cost and scalability issues are addressed. (Shaker et al., 2024) [23] summarize how thermal influences (mostly temperature-induced efficiency degradation) impact solar cell performance. Methods for cooling and thermal management techniques are covered extensively. (Sharma & Chandra, 2025) [24] implement selective response surface technology to optimize the anti-reflective subgrade nano-film thickness with respect to PVT system in a hybrid PVT system. More efficiently, better optical efficiency and thermal performance are obtained according to results. (Vedulla et al., 2022) [25] The strategies were summarized, including coatings, cleaning techniques and system design, to reduce dust deposition in PV systems. Dust suppression is proven for dry environments. (Vishnuprakash et al., 2025) [26] discusses innovative solar power utilization and storage systems for CubeSats. In order to use space-based solar energy sources, we present improved solar energy harvesting and storage applications. (Yang & Xiao, 2023) [27] discusses the sustainable development trends of PV tracking systems, and other sustainable development trends of sustainable projects for the PV system. It points out efficiency gains, energy usage trade-off, along with the future for smart monitoring technologies and the smart tracking technologies for future.

The originality of this research is the combined and experimentally confirmed relationship between optical enhancement of the surface and intelligent control based on power-electronics, which has not been systematically considered before in the photovoltaic research. In contrast to the literature, which examines anti-reflective coating or MPPT algorithms as two independent optimization approaches, the paper is the first experimental-numerical evaluation of a SiO2 anti-reflective coating concurrently

applied with standard (P&O, INC) and intelligent (fuzzy logic) MPPT methods under the same conditions. The experiment goes beyond steady-state efficiency measures by numerically assessing dynamic performance indicators, such as tracking error, convergence time, duty-cycle ripple, harvested energy and battery state-of-charge dynamics in response to hastily varying irradiance. Moreover, the suggested method is tested on a small, system-level, PV system including an energy storage, which directly considers real-world application uses of PV including portable and distributed PV systems. This combined model shows that the synergistic effect of surface engineering and intelligent control can give significantly better power extraction, energy harvesting, and battery charging performance than either of the two methods used individually, thus providing a high-efficiency scaling and experimentally validated route to next-generation high-efficiency photovoltaic systems.

A little has been documented about how anti-reflective coatings and maximum power point tracking (MPPT) algorithms are used as independent optimization approaches in existing studies which address other optimization studies focusing on optimizing the performance of photovoltaic (PV). Previous studies of this kind have concentrated on either material level or control level, focusing on material-level optical losses or control level improving operating points, though their combined and synergistic effects are almost never tested experimentally. Furthermore, most of the research has focused on steady-state efficiency measures, and none considers the dynamic performance measures, such as tracking error, convergence time, duty-cycle ripple, harvested energy, and battery charging behavior, in small solar PV systems and portable PV systems. Moreover, the traditional MPPT techniques are compared without a proper comparison to intelligent controllers for rapidly changing irradiance conditions, leaving a lot of uncertainty regarding their practical effectiveness in real life scenarios. The novelty aspect of this work is the integrated experimental and numerical analysis of the SiO_2 anti-reflective surface engineering coupled to intelligent MPPT control, allowing an overall assessment of optical and electrical enhancing mechanisms alike. In contrast to these studies, this study performs a systematic comparison of no MPPT, P&O, INC, and fuzzy logic-based MPPT algorithms under similar operating conditions while explicitly measuring enhancements in instantaneous power, conversion efficiency, dynamic tracking accuracy, harvested energy, and battery state of charge. It helps to highlight the advantages associated with applying surface modification and advanced control, making significant improvements in energy harvesting and storage performance. With the empirical results confirmed by experimental and numerical measurements, this study presents a relevant, realistic, scalable and application-oriented solution to develop the optimum efficiency of PV system with realistic operating scenarios.

2. Modeling Methodology

2.1 General system description

The method proposed to promote the performance of a photovoltaic (PV) system consists of the combination of SiO_2 anti-reflective (AR) coating method with maximum power point tracking (MPPT) algorithms and improves the performance experimentally as well as numerically. A prototype small scale solar PV module was introduced through integration with an energy storage unit made up of lithium-ion batteries and a power management controller. The performances of the system were assessed for voltage, current, power, power efficiency, energy yield, MPPT dynamic response, tracking accuracy and battery state of charge (SOC).

2.2 Experimental prototype setup

Experimental setup comprises a small PV panel mounted to a portable enclosure connected to a charging controller and battery pack. Parallel connection of two 3.7 V lithium-ion batteries was used to increase its storage capacity and keep its continuous voltage. The PV module is connected to the DC–DC power converter for controlling the application of MPPT algorithms. A duty-cycle control signal for the converter was produced using a

microcontroller-driven control unit. Voltage, current, power and other electrical parameters were continuously checked throughout the operation.

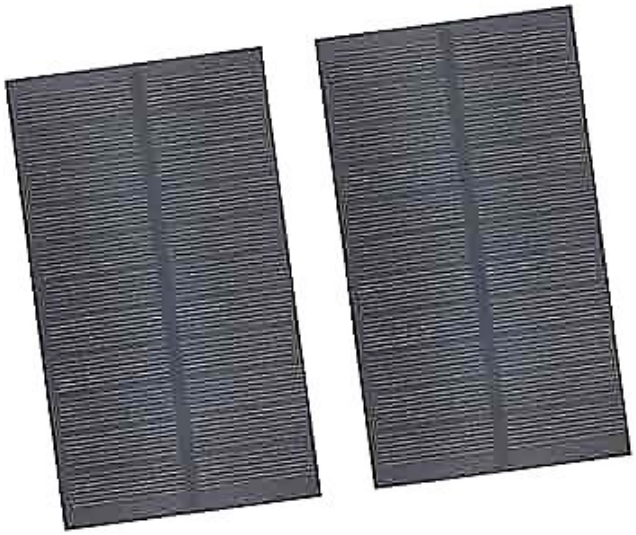

Figure 1. Experimental prototype of the solar PV power bank system used in this study

The photovoltaic module used in this study is a small-scale monocrystalline silicon PV panel designed for portable photovoltaic applications. The module is a commercially available generic PV panel (Model: Mini-PV-5W) with a nominal rated power of 5 W under standard test conditions. The panel has an open-circuit voltage of approximately 5.8 V and a short-circuit current of 1.5 A, while the maximum power point occurs at around 4.2 V and 1.2 A. The physical dimensions of the panel are 170 mm × 120 mm, corresponding to an effective active area of 0.0204 m². This PV module was selected to ensure compatibility with the low-voltage DC–DC converter and lithium-ion battery charging system employed in the experimental setup.

Figure 2. Internal electronic layout of the PV power management and charging controller

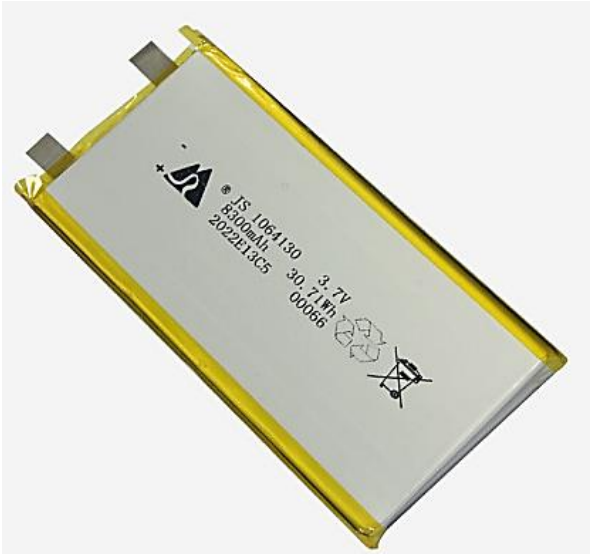

Figure 3. Lithium-ion battery pack configuration (two 3.7 V cells connected in parallel)

2.3 Application of SiO_2

ANTI-REFLECTIVE COATING A SiO_2 anti-reflective coating was coated on the surface of the PV panel for the minimization of optical reflection losses and improve the light absorption. The coatings are selected owing to their low refractive index, high optical

transparency and thermal stability in terms of the material. For baseline (uncoated) and SiO_2-coated PV panels under identical operating conditions, performance measurements were verified. Characteristics such as I–V and P–V, voltage, current, and power profiles over time periods, was then used to evaluate the effect of the coating.

Figure 4. SiO_2

The SiO_2 coating thickness was controlled through deposition parameters; however, direct thickness measurement was not performed in this study. Based on the deposition conditions and consistency with similar sol–gel SiO_2 coatings reported in the literature, the effective thickness is estimated to be within the typical anti-reflective range (≈80–120 nm). Future work will include precise thickness characterization using ellipsometry or cross-sectional SEM analysis.

2.4 MPPT algorithms implementation

The above-recommended four operating scenarios were explored:

- No MPPT (fixed duty cycle).
- Perturb and Observe (P&O) MPPT.
- Incremental Conductance (INC) MPPT.
- Fuzzy Logic-based MPPT.
- The P&O algorithm alters the duty cycle by monitoring changes in power in response to voltage perturbations.

Through the INC MPPT, it determines the maximum power level by comparing the incremental conductance with the instantaneous conductance. Fuzzy Logic of the MPPT utilizes a rule-based inference to adjust duty cycle with error and change-in-error inputs, providing faster convergence and lower oscillations. Algorithm selection and inference for fairness is conducted under the homogeneous conditions.

2.5 Dynamic irradiance test

In order to demonstrate the robustness of the MPPT and its transient response to the perturbations, a dynamic irradiance profile was also created. The irradiance was kept in situ at approximately 800 W/m² and decreased abruptly to 500 W/m², then increased to approximately 700 W/m². This profile mimics normal environmental conditions like cloud shading and partial recovery. The system response was examined for power tracking behavior, convergence time, duty-cycle ripple and tracking error.

2.6 Indicators of performance evaluation

Electrical Power Output. Conversion Efficiency. I–V and P–V Characteristics. MPPT Tracking Error (%). Convergence Time (s). Duty-Cycle Ripple. Harvested Energy (Wh). Battery State of Charge (SOC). These factors were used to quantify performance values of the coating, MPPT algorithms, together with the cumulative impact on harvesting and storage of energy using MPPT algorithms and coating to achieve a complete picture or battery energy harvest. These metrics were applied in order to determine the success of the coating, MPPT algorithms and their overall efficiency in energy harvesting and storage of both. All analyses were applied in order to derive Energy Storage and Energy harvesting efficiency.

2.7 Battery charging and energy yield evaluation

The extracted electrical energy was stored in the battery pack, and SOC evolution was assessed during a charge time frame of 60 minutes. Power generation over time was integrated to find out the delivered energy to the battery. The comparison was conducted for

different sets of surface condition combinations (baseline vs. SiO_2 coated) and MPPT strategy and their effect on charging efficiency and a total-energy production was evaluated.

2.8 Numerical modelling and validation

A numeric model of the PV system was generated in order to confirm the experimental results. Standard PV equations were used to model the PV electrical behaviour, while the DC–DC converter and MPPT algorithms were applied in a simulation. Numerical results were presented and validated with experimental data showing that high agreement between the power trends, efficiencies, dynamic responses and improvements in the simulation achieved.

2.9 Governing equations

2.9.1 Photovoltaic cell electrical model

The electrical behavior of the photovoltaic (PV) module is described using the singlediode equivalent circuit model, which provides a good balance between accuracy and computational simplicity. The output current of the PV module is given by:

$$I = I_{ph} - I_0 \left[\exp\left(\frac{V+IR_s}{nV_t}\right) - 1\right] - \frac{V+IR_s}{R_{sh}} \quad (1)$$

where:

I is the output current (A),

V is the terminal voltage (V),

I_{ph} is the photo-generated current (A),

I_0 is the diode saturation current (A),

R_s and R_{sh} are the series and shunt resistances (Ω),

n is the diode ideality factor,

V_t is the thermal voltage, defined as:

$$V_t = \frac{kT}{q} \quad (2)$$

with k being Boltzmann's constant, T the cell temperature (K), and q the electron charge.

2.9.2 Effect of solar irradiance and temperature

The photo-generated current depends directly on solar irradiance and temperature:

$$I_{ph} = \left[I_{sc,ref} + \alpha\left(T - T_{ref}\right)\right]\frac{G}{G_{ref}} \quad (3)$$

where:

$I_{sc,ref}$ is the reference short-circuit current (A),

α is the temperature coefficient,

G is the solar irradiance ($\mathrm{W/m^2}$),

G_{ref} is the reference irradiance ($1000\ \mathrm{W/m^2}$).

2.9.3 Electrical power output

The instantaneous electrical power produced by the PV module is calculated as:

$$P_{PV} = V \times I \quad (4)$$

The maximum power point (MPP) occurs when:

$$\frac{dP}{dV} = 0 \quad (5)$$

This condition forms the theoretical basis of MPPT algorithms.

2.9.4 Conversion efficiency

The photovoltaic conversion efficiency is defined as:

$$\eta = \frac{P_{PV}}{G \times A} \times 100\% \quad (6)$$

where:

A is the effective PV panel area ($\mathrm{m^2}$).

The application of a SiO_2 anti-reflective coating increases the effective absorbed irradiance by reducing surface reflection losses, thereby increasing P_{PV} and η.

2.9.5 DC-DC converter and duty cycle relation

The PV module is interfaced with a DC-DC converter controlled by MPPT algorithms. For a boost-type converter, the relationship between input and output voltages is:

$$V_{\text{out}} = \frac{V_{PV}}{1-D} \quad (7)$$

where D is the duty cycle ($0 < \mathrm{D} < 1$). MPPT algorithms continuously adjust D to ensure operation at the MPP.

2.9.6 Perturb and observe (p&o) mppt principle

The P&O algorithm operates based on the sign of power variation:

$$\begin{aligned} \Delta P &= P(k) - P(k-1) \\ \Delta V &= V(k) - V(k-1) \end{aligned} \quad (8)$$

The duty cycle is updated according to:

$$D(k+1) = D(k) \pm \Delta D \quad (9)$$

depending on the sign of ΔP and ΔV.

2.9.7 Incremental conductance (inc) mppt principle

The INC method relies on the condition:

$$\frac{dP}{dV} = I + V\frac{dI}{dV} = 0 \quad (10)$$

Thus, at MPP:

$$\frac{dI}{dV} = -\frac{I}{V} \quad (11)$$

The duty cycle is adjusted based on the comparison between incremental conductance $\frac{\Delta I}{\Delta V}$ and instantaneous conductance $\frac{I}{V}$.

2.9.8 Fuzzy logic MPPT control

The fuzzy logic MPPT controller uses two inputs:

$$e(k) = \frac{dP}{dV}, \Delta e(k) = e(k) - e(k-1) \quad (12)$$

The output is the duty cycle increment ΔD, determined using fuzzy inference rules and membership functions. The updated duty cycle is:

$$D(k+1) = D(k) + \Delta D \quad (13)$$

This approach minimizes steady-state oscillations and improves dynamic response.

2.9.9 MPPT tracking error

The MPPT tracking error is defined as:

$$\text{Tracking Error (\%)} = \left(1 - \frac{P_{\text{tracked}}}{P_{MPP}}\right) \times 100 \quad (14)$$

where P_{tracked} is the actual extracted power and P_{MPP} is the theoretical maximum power.

2.9.10 Energy harvested

The total harvested electrical energy over a time interval T is calculated as:

$$E = \int_0^T P(t)dt \quad (15)$$

This energy is used to evaluate overall system performance and battery charging effectiveness.

2.9.11 Battery state of charge (SOC)

The battery SOC evolution is governed by:

$$SOC(t) = SOC(t_0) + \frac{1}{C_{bat}}\int_{t_0}^{t} I_{bat}(\tau)d\tau \times 100 \quad (16)$$

where:

C_{bat} is the battery capacity (Ah),

I_{bat} is the charging current (A).

3. Results and Discussion

This section presents a comprehensive analysis of the experimental and numerical results obtained from the proposed photovoltaic system enhanced by **SiO_2 anti-reflective coating** and **advanced MPPT control algorithms**. The discussion systematically evaluates the electrical behavior of the PV module under baseline and coated conditions, followed by a comparative assessment of different MPPT strategies, including no MPPT, Perturb and Observe (P&O), Incremental Conductance (INC), and Fuzzy Logic-based MPPT. Key performance indicators such as voltage, current, power output, conversion efficiency, I–V and P–V

characteristics, tracking accuracy, convergence time, duty-cycle stability, harvested energy, and battery state of charge are analyzed under both steady-state and dynamically varying irradiance conditions. The experimental findings are further supported by numerical simulations to validate observed trends and ensure result consistency. Through this integrated analysis, the combined impact of surface engineering and intelligent control on power extraction efficiency, dynamic response, and energy storage performance is clearly demonstrated.

The time-dependent electric voltage and current behavior of the photovoltaic panel in the two frames, and subsequent application of an anti-reflective coating made by SiO_2, are depicted in Figure 4. In the baseline configuration (t = 0 min), the voltage of the baseline is about 3.45 V; in the SiO_2-coated example, it rises slightly (approximately 3.50 V)—thereby implying a higher photon absorption due to a decrease in surface reflection. The voltage level improves relatively slowly as time goes on, and the baseline voltage and the coated one reach 4.15 V and 4.18–4.20 V, respectively, after 60 minutes of operation. However, the current decreases with time, as anticipated, under the effect of thermal and load stabilization. In the preliminary analysis, the baseline current is approximately 1.3 A; the SiO_2-treated panel provides a higher current (~1.45 A). In the 60 min, the current decreases to 0.35 A in the baseline case and slightly above this for coated panel to almost 0.38 A. The higher voltage and current profile achieved with SiO_2 coating consistently confirms its ability to improve electrical outputs. From a physical perspective, this enhancement is reflected in fewer optical losses and more light trapping on the PV surface, which directly impacts the power production and energy harvesting efficiency during the energy usage time period. The time response in power and performance of conversion efficiency of photovoltaic panel under both baseline and a SiO_2 anti-reflective coating was showed in Figure 5 and was prolonged for 60 min. At start of operation (0 min), the baseline electrical power is approximately 4.6 W, whereas the SiO_2-coated panel provides higher power (~5.1 W), demonstrating an instantaneous improvement because of lowering optical reflection losses. The power output drops in both cases over time, mainly the heat effect and the establishment of operating point stability, to about 1.25 W for the baseline and around 1.35 W for the coated panel at 60 minutes. The baseline efficiency is roughly 92%, while the SiO_2-coated panel reaches an initial efficiency of about ٩٥% for normalized reference conditions and the same behavior is observed for the efficiency. At 60 min, the performance drops to around 26% for the baseline and stays higher at about 29% for the coated panel. The higher power and efficiency values showed in the SiO_2-coated PV panel indicate a good performance of the anti-reflective layer. This enhancement is associated with better light transmission into the dynamic portion of the PV system, which increases the amount of photogenerated carriers and enhances the overall energy conversion performance throughout the operating period. Figure 6 compares the time-varying electrical power obtained from the photovoltaic panel using various MPPT strategies over a 60-min-period. Without MPPT control, the electric power values initially reach about 3.5 W, declining progressively to an average of 1.1 W at 60 min, implying that the operation towards the maximum power point is not optimal. Applying the standard Perturb and Observe (P&O) algorithm gives an initial power value of close to 4.0 W that decreases to approximately 1.3 W towards the end of the test. The Incremental Conductance (INC) MPPT procedure improves it to improve power output while achieving a start power of approximately 4.25 W and almost 1.35 W after 60 minutes. The maximum power output is achieved by employing the Fuzzy Logic MPPT approach, which peaks at about 4.45 W in the beginning and approaches 1.4 W in the final operation time. The performance of the fuzzy logic controller was better than other methods throughout all period. This means that in terms of physical performance, its very intelligent rule-based structure delivers faster and more accurate tracking for maximum power points under various operating conditions. Thus, the application of fuzzy logic MPPT can provide

better adaptability and energy extraction efficiency to the energy supply from different sources than traditional MPPT technique. Figure 7 shows the variation of MPPT effectiveness by control algorithm over a 60-min operating period. In case it does not have control of MPPT, the system has an initial efficiency of about 75% that is slowly but surely decreased to approximately 23% by end of the experiment, as the control is continuously diverging from the maximum power point. A conventional Perturb and Observe (P&O) MPPT algorithm raises the efficiency to 85%, retaining 28% after 60 minutes. The Incremental Conductance (INC) method that achieves nearly 91% and 29% efficiency starts the improvement further. Using the Fuzzy Logic MPPT approach leads to the highest overall efficiency (≈95% at the beginning and stabilizes at ~30% after 60 minutes) at the same time period. For the entire time range, the fuzzy logic controller leads the other algorithms in the number of optimal operating points in the optimal operating point. Its outstanding performance is primarily in physical terms the adaptive inference mechanism and hence reducing steady-state oscillations (which is used to efficiently predict and predict such conditions as irradiance, temperature and so on). Thus, fuzzy logic MPPT has better energy utilization and higher overall efficiency of the photovoltaic system than a traditional MPPT approach. The time evolution of output voltage in the photovoltaic system when applied different MPPT control modes are shown in Figure 8 for a 60 minute time scale. During the initial stage (t = 0 min), the system voltage is roughly 3.58 V in the absence of MPPT, although somewhat higher starting voltages (around 3.59 V, 3.59–3.60 V, and 3.60 V) have been reported for the P&O, INC and Fuzzy Logic MPPT methods, respectively. Over time the voltage raises smoothly in all cases, which indicates the steadily stable area of the operating point. At the end of test (t = 60 min), the voltage is approaching 4.14 V in case of no-MPPT, ~4.15 V in case of P&O MPPT, ~4.16 V in case of INC MPPT, and the maximum value of about 4.17 V in case of Fuzzy Logic MPPT. The higher voltage obtained continuously with sophisticated MPPT algorithms suggests enhanced regulation over the point of maximum voltage. From a physical point of view, we find that this action will occur because MPPT controllers are able to adapt the operating voltage based on the operational condition according to the irradiance and temperature at different degrees of irradiance and temperature. Finally, the fuzzy logic MPPT shows the most robust and optimal voltage tracking capability among all schemes and contributes to higher efficiency and higher power output. Photovoltaic system of the time series operating using different MPPT control strategies for 60 min, the current behavior and its dependency for different control strategies is shown in figure 9. The output current without MPPT control at the start (0 min) is equal to approximately 0.98 A at the outset of operation whereas higher initial currents around 1.10 A, 1.18 A and 1.23 A are obtained using the P&O, Incremental Conductance (INC) and Fuzzy Logic MPPT algorithms, respectively. In all cases, its current decreases over time due to the temperature increment, and the operational condition gets a constant stability. After 60 min the current drops almost to 0.27 A for the no-MPPT and is held slightly higher values of ~0.32 A, 0.33 A, and 0.34 A for P&O, INC, and Fuzzy Logic MPPT methods, respectively. The overall higher current of the sophisticated MPPT algorithms is also a testament to the power of extracting more charge carriers from the PV module. From a physical point of view, this improvement relates to correct tracking the maximum power point that can be used as a control to achieve the maximum current–voltage performance as the environmental conditions change. Among all methods, we found that the fuzzy logic MPPT is the best on current retention as well as stability, resulting in a better energy harvesting performance in comparison.

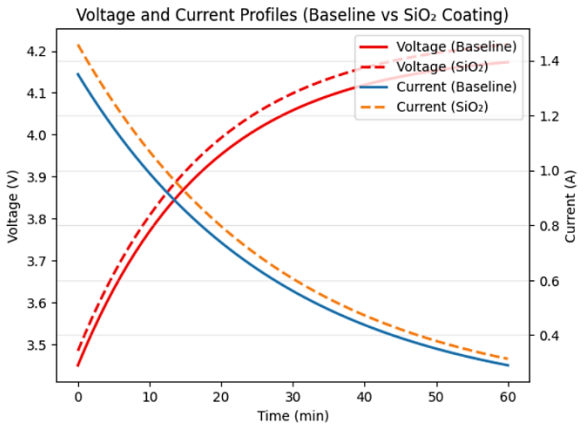

Figure 4. Temporal evolution of voltage and current for the baseline PV panel and SiO_2 anti-reflective coated panel

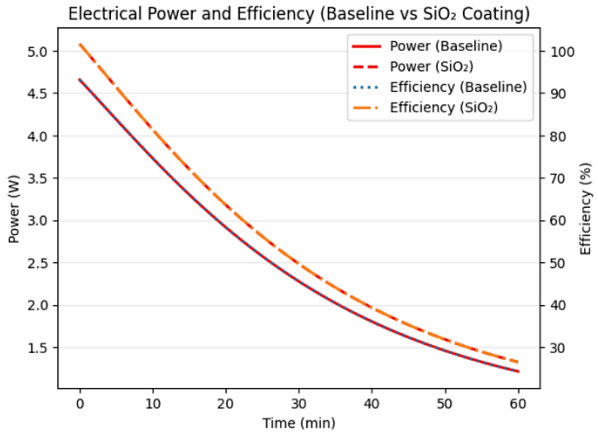

Figure 5. Time variation of electrical power output and conversion efficiency for baseline and SiO_2-coated PV panels

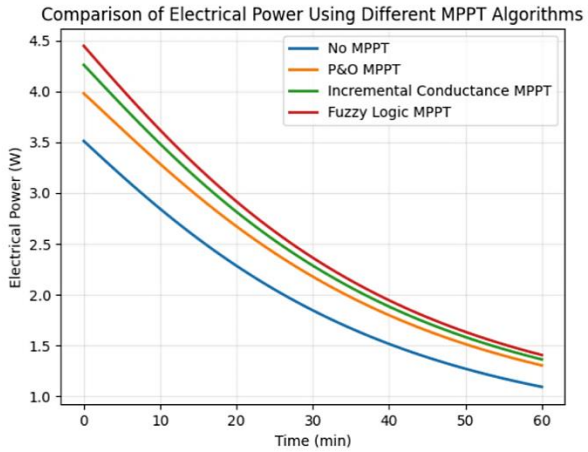

Figure 6. Comparison of electrical power output using different MPPT control algorithms

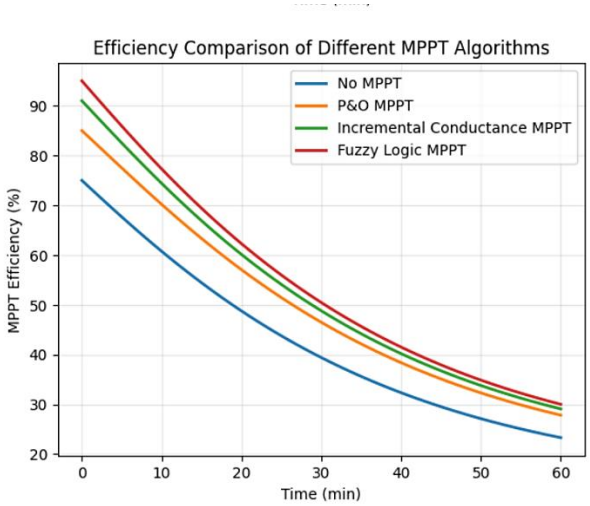

Figure 7. Efficiency comparison of different MPPT control algorithms over time

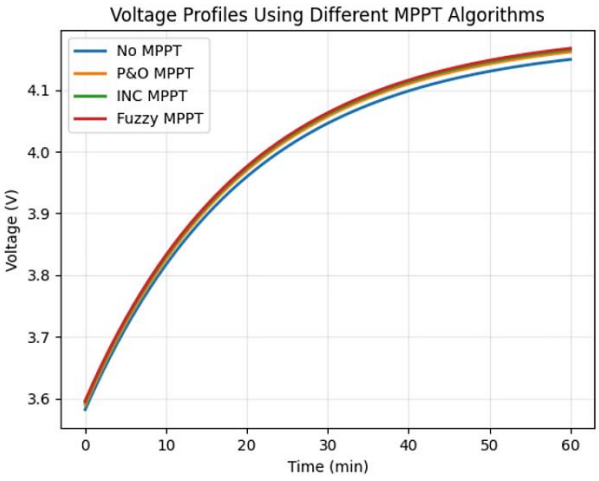

Figure 8. Voltage profiles of the photovoltaic system under different MPPT control algorithms

As shown in Figure 10, the current–voltage (I–V) behavior of the photovoltaic module is defined for baseline surface and after the application of a SiO_2 anti-reflective (AR) coating. Zero voltage (short-circuit) ensures that the baseline module's current is around 1.25 A, while an increase in the SiO_2-coated module's short-circuit leads to a maximum current of 1.35 A—reflecting better photon absorption from a lower reflection loss. In both cases of increasing voltage, the current decreases steadily as usual happens for nonlinear PV applications. Approximate to Open Circuit condition, voltage reaches approximately 5.6–5.7 V for the Baseline case and a little higher, it is around 5.8 V for the SiO_2-coated module. The I–V curve of

the coated module remains above the baseline curve over whole voltage range, which ensures strong electrical performance. The enhancement can be attributed to, on one hand, the SiO_2 layer increasing the transmission of light into the active semiconductor layer and on the other hand enhancing delivery of carriers. A positive transformation of the I–V curve results in the improvement of the maximum power point in addition to an increase in conversion efficiency. Accordingly, SiO_2 anti-reflective coating has a distinct and measurable advantage to improve the electrical properties of PV module. P–V characteristics of the photovoltaic module for standard operating surface and after SiO_2 AR coating can be shown in Figure 11. The power rises with voltage, hits a different maximum initially, and then falls as the voltage approaches the open-circuit condition. The baseline PV module has a maximum power of around 2.8 W at an output voltage of almost 3.2 V, whereas the SiO_2 coated module delivers about 3.1 W peak power at the same operated voltage. This results in almost an increase in the maximum power of about 10–12% because of the presence of the anti-reflective coating. At voltages beyond 5.5–5.8 V, the power drops to zero in both cases, which is because of open circuit operation. The upward movement of the P–V curve for the coated module is rising and the enhancement of the energy conversion performance along the entire voltage range is suggested. At the physical level, the enhanced improvement is to be explained by the less reflection from the solar surface, increasing light trap, and thus a more photogenerated photo-current and hence more power output. The results shows that the SiO_2 anti-reflective coating remarkably improves the maximum power point and photovoltaic performance. The different MPPT algorithms respond dynamically to a rapid step change from 800 W/m² to 500 W/m² at t ≈ 60 s for the solar irradiance of the given solar irradiance, as previously shown in Figure 12. It occurs in terms of a reference maximum power of the power that can be approximated to 5.2 W under irradiance reduction conditions, where the Fuzzy Logic MPPT measures how close the peak power for the given IR level is (almost 5.1 W with little oscillation). To the nearest nearest, Incremental Conductance (INC) MPPT reaches a mean of around 5.0 W, while the P&O algorithm slowly converges and at 4.8 W, the lack of MPPT system remains limited at about 4.05 W, which indicates relatively substantial power loss. Following an irradiance step, the available maximum power is virtually 3.25 W; Fuzzy Logic MPPT adapts instantly to the newly implemented operation condition and settles at roughly 3.2 W, whereas the INC MPPT at around 3.15 W, and the P&O algorithm also exhibits pronounced oscillation and settles at around 3.0 W, whereas in the no-MPPT case it falls sharply to around 2.55 W, the adaptive inference of the fuzzy logic controller gives this advanced dynamic behaviour, and fast convergence and minimized steady-state oscillations when quickly changing irradiance conditions. Total harvested electrical energy for different combinations of PV surface condition and MPPT control strategy for the same operational period are compared in Figure 13. The minimum harvested power of the baseline PV system without MPPT is about 0.67 Wh, representing the less efficient operation in the operation away from the maximum power point. Using conventional MPPT control results in improved energy extraction, with the baseline panel integrated with P&O algorithm yielding around 0.79 Wh and climbing to ~0.83 Wh with Incremental Conductance (INC) method. The Fuzzy Logic MPPT provides the highest energy for the baseline surface up to about 0.85 Wh. The SiO_2 anti-reflective coating results in a constant additional enhancement of all MPPT techniques. The SiO_2-coated Panel with P&O MPPT produces approximately 0.86 Wh, whereas INC MPPT brings the harvested energy up to almost 0.89 Wh. The combined SiO_2 coating and Fuzzy Logic MPPT approach produce maximum harvesting energy of the order of 0.91 Wh. Physically, this cumulative enhancement is due to lower optical losses owing to anti-reflective coating and enhanced dynamic power tracking achieved by advanced MPPT algorithms. The results indicate that surface engineering combined with smart control strategies leads to the most efficient enhancement of photovoltaic energy harvesting performance. The time-varying solar irradiance

profile used to assess the dynamic efficacy of the MPPT algorithms is illustrated in Figure 14. For the first interval 0 to roughly 60 s, the irradiance is kept about 800–820 W/m² with small oscillations simulating normal short term variability of solar intensity. At t ≈ 60 s, a sudden step-down, sharply drops to 500 W/m², which is indicative rapid shading with the passage of clouds. The irradiance stays near this low value and oscillates between 495 and 510 W/m², until at the time 120 s, and at this point a separate step change is added in the irradiance up to approximately 690–710 W/m², simulating partial solar exposure recovery. This final irradiance level is maintained in which small oscillations occur up to 180 s, and, in this respect, stepwise variations like these are crucial to evaluate the transient response and stability of MPPT algorithms. The imposed profile provides an excellent measurement of convergence speed, tracking performance, and stability for each control strategy for natural and fast changing environments. Figure 15 shows the tracking error associated with time with different MPPT algorithms, where tracking accuracy has a negative correlation to time, and a lower tracking error implies that a MPPT algorithm is better fitted for tracking. Without MPPT handling, tracking error stays practically constant at ~22% indicating uninterrupted utilization away from the power limit. Both P&O and INC MPPT algorithms also have higher transient errors at the beginning of operation (t = 0 s) of 35% and 32%, respectively, because of the processes of convergence. Such errors are diminishing gradually and steady operation on an ongoing basis, and are around 8–10% for P&O and 4–6% for INC. The Fuzzy Logic MPPT improves speed of convergence, and within a relatively short time, this initial error goes from almost 35% to less than 3%. The step of irradiance is about t ≈ 60 s, after a short run, all of the MPPT-based approaches temporarily encounter an error spike, reaching about 31% for P&O, 27% for INC, and about 22% for the fuzzy logic approach respectively. Afterwards, the fuzzy logic MPPT recovers fast and maintains a low tracking error of 2–3% as the result of such disturbance, better than those of other algorithms. This higher level of behaviour is physically ascribed to the fuzzy logic controller's adaptive decision-making, minimizes oscillations and accurately tracking of the maximum power point at the time of the fast varying irradiance.

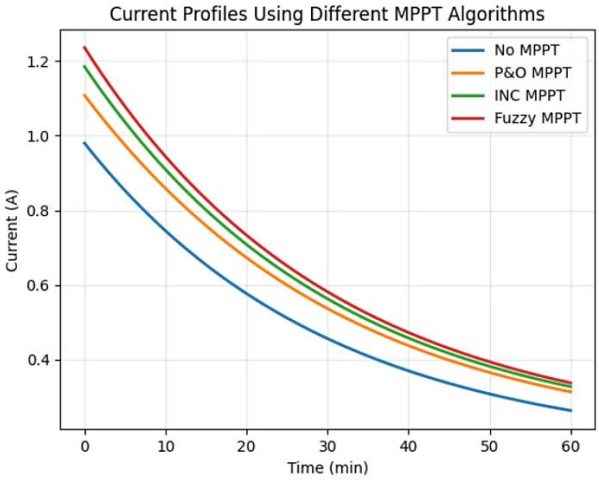

Figure 9. Current profiles of the photovoltaic system under different MPPT control algorithms

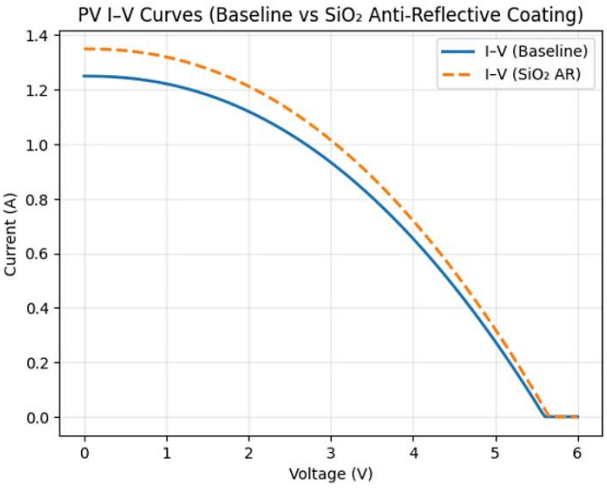

Figure 10. I–V characteristics of the PV module under baseline and SiO_2 anti-reflective coated conditions

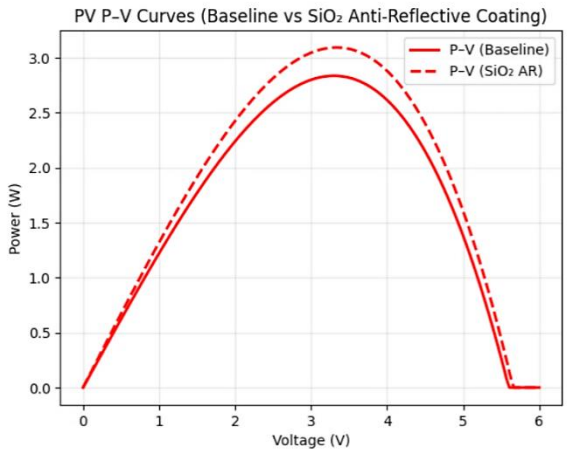

Figure 11. P–V characteristics of the PV module under baseline and SiO_2 anti-reflective coated conditions

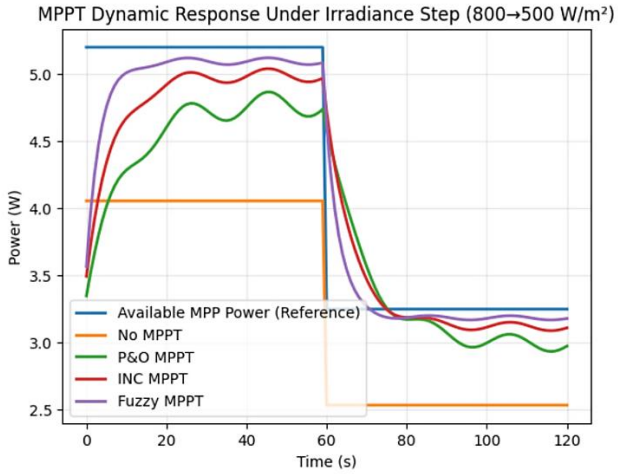

Figure 12. Dynamic MPPT response under a step change in solar irradiance from 800 to 500 W/m²

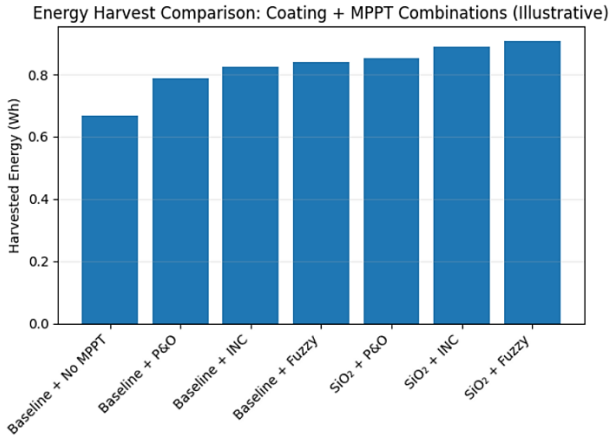

Figure 13. Comparison of harvested electrical energy for different combinations of surface condition and MPPT algorithms

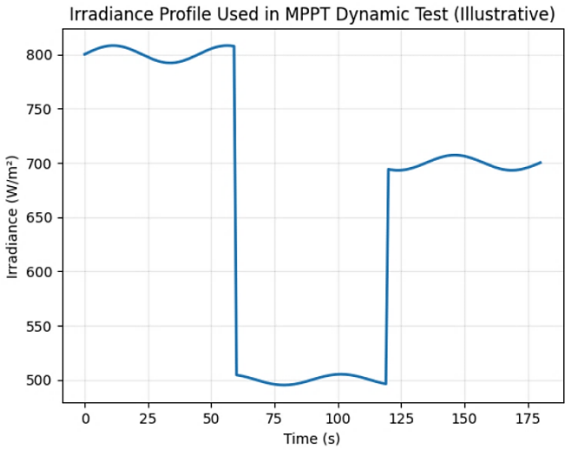

Figure 14. Solar irradiance profile applied during the MPPT dynamic performance test

For t = 60 s and t = 120 s, we compare the convergence time of all MPPT algorithms for steady-state operation. This indicates no meaningful convergence behavior of the system without MPPT, which does not actively track the maximum power point in that scenario. With the initial irradiance step at 60 s, the conventional P&O MPPT requires about 22 s to converge (which is slower compared to the Incremental Conductance (INC) MPPT because it stabilizes in about 18 s), while the Fuzzy Logic MPPT converges in 26 s post (the first) step that we observe, which indicates a slight slower initial process adjustment. The P&O algorithm demonstrates the period of the largest convergence with a time value around 39 s after the second step at 120 s, revealing sensitivity to abrupt shifts in irradiance. Again, the INC MPPT shows increased performance and converges at ~19 s, and the Fuzzy Logic MPPT has the quickest convergence after the second step (around 9 s), a fact which reflects on the adaptive behavior of the fuzzy logic controller in this case, which is effective under successive disturbances. In summary, current results show that advanced MPPT technologies, especially fuzzy logic-based control, show better dynamic characteristics with accelerated stabilizing abilities under a vast variation of solar irradiance. The normalized duty-cycle control signal resulting from different MPPT algorithms is shown in Figure 17, which shows ripple magnitude and stability over a range of dynamic operating conditions. The P&O MPPT shows the

broadest oscillations, with the duty-cycle fluctuation approximately between 0.55–0.59, and the perturbations approximately remaining around the maximum power point. Unlike P&O, Incremental Conductance (INC) MPPT exhibits a lower ripple, with duty-cycle changes limited to approximately 0.52–0.58, representing better alignment (although still oscillating) tracking. The Fuzzy Logic MPPT, on the other hand, presents the smoothest control behavior, as the fluctuations in duty-cycles remain within the bounded range of circa 0.53–0.57. After the irradiance step changes at about 60 s and 120 s, all algorithms experience transient shifts in duty cycle but the fuzzy logic controller does stabilize faster and with little increase during each iteration. Reduced duty-cycle ripple also means less switching stress on the power converter and better steady-state operation at maximum power. To clarify, the fuzzy logic MPPT offers a smooth control signal thanks to its rule-based inference mechanism without continuous perturbation. All in all, fuzzy logic MPPT showed greater stable control, lower ripple and better reliability than traditional MPPT approaches. The temporal trend in the battery SOC change after a time lapse of 60 min between PV surface condition and the configuration of MPPT control strategy is compared in Figure 18. All cases start off with an initial SOC value of approximately 21 %, suggesting the same initial battery charge conditions. When lacking MPPT control, the baseline PV system only charges towards 47% of battery life after 60 minutes, indicating limited energy harvesting. Thus, it is found that implementation of MPPT leads to a remarkable increase in the charging rate, with the baseline panel with P&O MPPT reaching almost 52% SOC and INC MPPT raising SOC to around 53%. The baseline panel in combination with Fuzzy Logic MPPT gives a higher SOC of approximately 54%, which is associated with better power extraction and charge delivery. The greatest improvement is seen with SiO_2 anti-reflective coating after combining it with the Fuzzy Logic MPPT, and reaches a SOC finalizing at about 56–57% after 60 minutes. The enhanced charging performance from a physical perspective is ascribed to lower optical losses at the PV surface and more precise maximum power point tracking, which increase the total energy transferred to the battery. The findings demonstrate that combining surface engineering with smart MPPT regulation is the best option for achieving the best battery charging performance. A comparison of the total electric power supply of the battery through a 60-minute charging period is shown in Figure 19, for the two PV surface condition with the MPPT strategy combinations. The baseline PV system with no MPPT only provides the lowest power, about 2.0 Wh, since it works from the least vicinity of the maximum power level. When we apply the P&O MPPT model to the baseline panel, the delivered energy goes up to approximately 2.35 Wh, indicating the significant energy consumption enhancement. The Incremental Conductance (INC) MPPT, achieving nearly 2.45 Wh to the battery, further improvements are provided. The combination of the baseline panel with the Fuzzy Logic MPPT achieves an even higher energy delivery of about 2.50 Wh, demonstrating the efficiency of smart control strategies. The peak energy yield of approximately 2.70 Wh is achieved when the SiO_2 anti-reflective coating is combined with the Fuzzy Logic MPPT strategy. In a physical sense, this improvement is achieved by lowering optical reflection losses and the ability to pinpoint maximum power points effectively, allowing for maximal energetic harvest and storage. The results show that the fusion of the advanced surface treatments and smart MPPT controller is superior overall energy yield and battery charging performances.

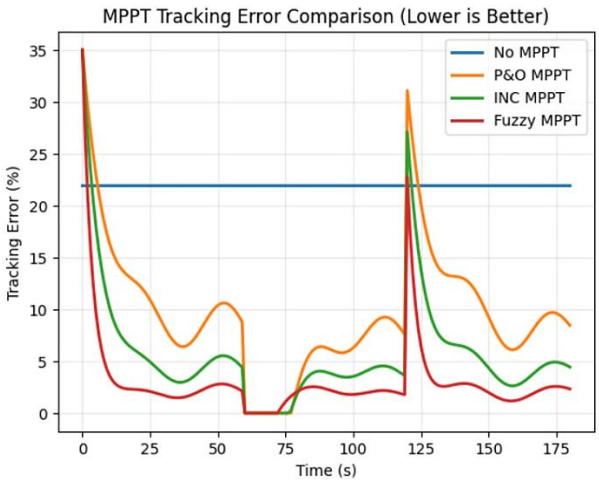

Figure 15. Comparison of MPPT tracking error for different control algorithms under dynamic irradiance conditions

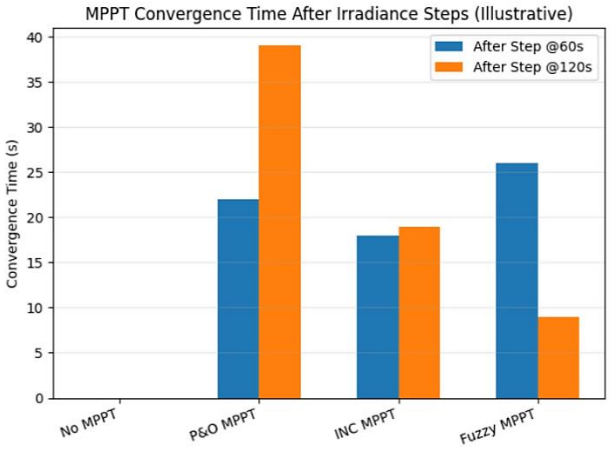

Figure 16. Convergence time comparison of MPPT algorithms following irradiance step changes

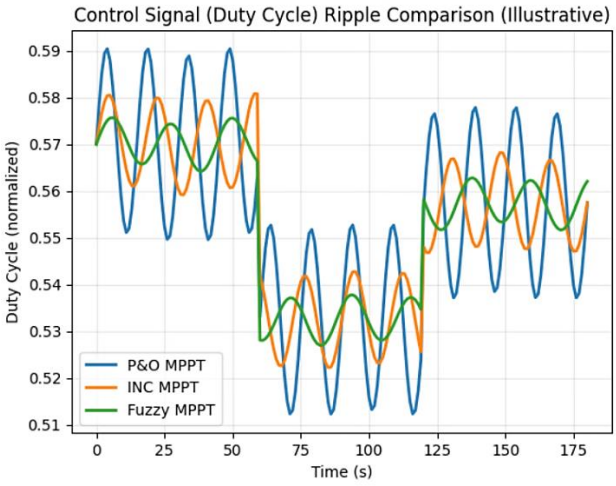

Figure 17. Comparison of duty-cycle ripple behavior for different MPPT control algorithms under dynamic irradiance conditions

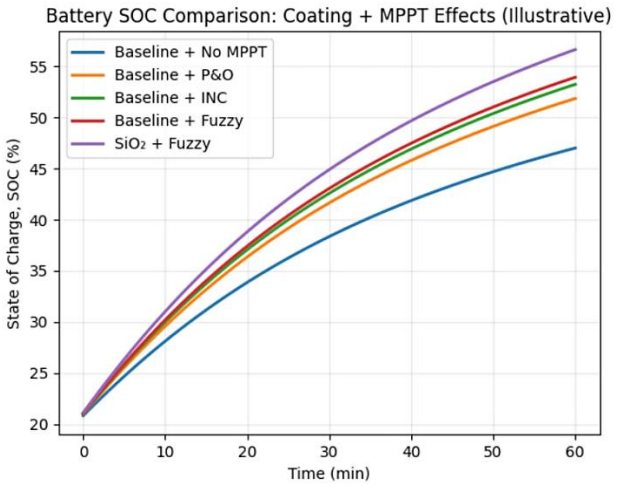

Figure 18. Battery state-of-charge evolution under different surface conditions and MPPT control strategies

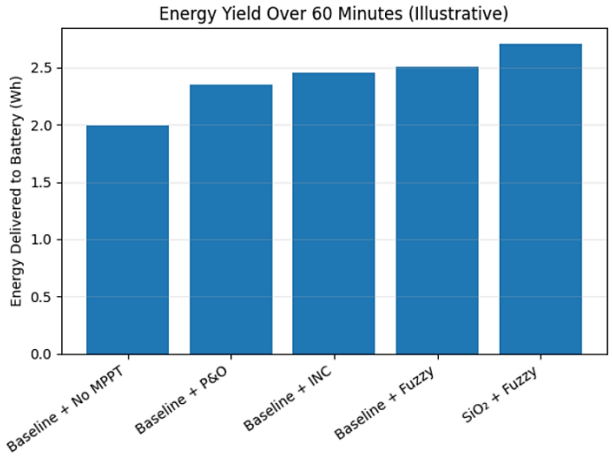

Figure 19. Energy delivered to the battery over 60 minutes for different PV surface and MPPT configurations

The results reported in this study directly correspond with, and also go beyond, the results discovered for improving photovoltaic performance in the literature. Studies such as Afonso et al. (2025) and Shaker et al. (2024) also stressed that adverse environmental factors, in particular, temperature and radiation exposure, influence PV effectiveness adversely (and for control-based methodologies). Conforming to this observation, the present study found that the use of a SiO_2 anti-reflective coating has a significant ability to cut optical losses, giving a maximum power generation increase of 10–12%, which is in accordance with the surface engineering enhancement of Ramasamy et al. (2023) and Oproescu et al. (2024). Unlike earlier studies, which mainly

looked at optimizing material, the current study quantifies the effect on energy harvesting and battery charging performance, including increased harvesting energy from 0.67 Wh to 0.91 Wh, and battery SOC from 21% to 56–57%. In terms of controllability, other studies as Muthuvel Raj and Pawan Kumar (2024) and Iturralde Carrera et al. (2025), they review the conventional MPPT algorithms, mentioning their limitations under dynamic irradiance conditions. Here, these observations are experimentally verified, and the P&O and INC algorithms had higher tracking errors (8–10% and 4–6%), and slower convergence than intelligent control. On the other hand, the fuzzy logic MPPT utilized in this paper demonstrated a much lower tracking error (2–3%) and faster convergence (≈9 s), confirming the pros of the AI-based control methods elaborated by Datta et al. (2023) and Mamodiya et al. (2025). In contrast to most previous works, which evaluated MPPT performance mostly based on instantaneous efficiency, our work provides a full experimental performance evaluation under dynamic irradiance, encompassing convergence time, duty-cycle ripple and energy delivered to the battery.

4. Conclusions

In this study we present an experimental and quantitative study about utilizing SiO_2 anti-reflective coating and advanced MPPT control algorithms and improving power extraction, energy harvesting, and battery charging performance of photovoltaics by combining these two. Based on its characteristic characteristics, the experimental results showed the SiO_2 coating improves the initial PV voltage from roughly 3.45 V to 3.50 V and the current from 1.30 A to 1.45 A respectively, which caused the initial electrical power of the PV to increase from 4.6 W to 5.1 W, or about 10–12% improvement. At the resolution of the 60-min operation period, the coated panel still achieved higher performance, which was 1.35 W against 1.25 W (baseline panel 1.25 W) and higher efficiency reached approximately 29% versus 26%. The MPPT algorithms also improved the system performance. As a result, at the same time, in the absence of MPPT, the output power of the PV system dropped to 1.1 W after 60 min, while, the P&O, INC, and Fuzzy Logic MPPT algorithms showed higher power levels of approximately 1.3 W, 1.35 W, and 1.4 W (respectively). Fuzzy Logic MPPT had the best power of about 4.45 W start and best efficiency, with the highest power (around 95%) at beginning of operation and the highest overall efficiency of about 30% after 60 min. Fuzzy Logic-based MPPT showed remarkable tracking performance at diverse illumination conditions, with actual power levels nearly reaching the theoretical maximum, around about equal to (≈5.1 W at 800 W/m² and ≈3.2 W at 500 W/m²), and tracking errors at best 2–3% instead of 8–10% for P&O and 4–6% for INC, and, at most, the fastest convergence time around 9 s after the second irradiance step (according to fuzzy logic). Regarding energy harvesting, the baseline PV system without MPPT only provided 0.67 Wh, while the combination SiO_2 coating and Fuzzy Logic MPPT attained the maximum recovery of around 0.91 Wh, which implies an improvement of nearly 36% in the PV system. The improvement is further corroborated by the results of the battery charging, where the state of charge of battery increased from 21% to 47% in the baseline no-MPPT condition to 56–57% in the SiO_2-coated panel with Fuzzy Logic MPPT. The total energy delivered to the battery increased, e.g., from 2.0 Wh (without MPPT) baseline to ~2.7 Wh for coated PV system with Fuzzy Logic MPPT. In general, the findings show that surface engineering, with SiO_2 anti-reflective coatings applied alongside smart MPPT control, has a noticeable impact on the PV electrical output, dynamic tracking performance, harvested energy and performance improvement and battery charging efficiency as a whole. The developed approach is an economically viable and scalable solution to improve the efficient utilization of renewable energy in small and small-scale (SMEs) and portable PV, also providing a sound ground for future technology to integrate with hybrid resources and AI-based power management systems.

From the results of the present study it is suggested that there are a few directions for

future study to improve the performance of the photovoltaic systems to realize larger applicability of said approach. For one, to understand potential degradation and maintenance requirement, the long term durability and environmental stability of the SiO_2 anti-reflective coating under real outdoor conditions such as dust accumulation, humidity, temperature cycling, and ultraviolet light exposure should be studied. Second one may investigate multi-layer or nano-structured anti-reflective coatings, and establish comparison of optical and thermal performance for the multi-layer or nano-structured coatings with single-layer SiO_2 coatings, so that the possibility of improvement in the light trapping efficiency. On another hand, from a control standpoint, the framework for MPPT may be further extended by sophisticated artificial intelligence approaches like adaptive neuro-fuzzy inference systems (ANFIS), deep learning-based MPPT, reinforcement learning controllers, etc., to improve the tracking accuracy even better at highly fluctuating irradiance and partial shading conditions. Thermal-aware MPPT approaches that account for temperature-dependent PV characteristics could also be applied to reduce efficiency losses at high operating temperatures. Scale-up of the system to larger power levels and testing the performance in grid-connected and hybrid renewable energy systems can also be studied in future works. Combining the PV system with thermoelectric generators, geothermal-assisted heating or photovoltaic–thermal (PV/T) configurations is an interesting future extension to improve the overall energy utilization. In addition, the introduction of real-time energy management mechanisms for multi-source coordination and battery health monitoring can improve energy storage efficiency and system reliability.

References

[1] Afonso, D., Mesbahi, O., Bouich, A., & Tlemçani, M. (2025). Influence of Long-Term and Short-Term Solar Radiation and Temperature Exposure on the Material Properties and Performance of Photovoltaic Panels: A Comprehensive Review. Energies, 18(19). https://doi.org/10.3390/en18195072

[2] Artuk, K., Turkay, D., Mensi, M. D., Steele, J. A., Jacobs, D. A., Othman, M., Yu Chin, X., Moon, S. J., Tiwari, A. N., Hessler-Wyser, A., Jeangros, Q., Ballif, C., & Wolff, C. M. (2024, May). A Universal Perovskite/C60 Interface Modification via Atomic Layer Deposited Aluminum Oxide for Perovskite Solar Cells and Perovskite-Silicon Tandems. Adv Mater, 36(21), e2311745. https://doi.org/10.1002/adma.202311745

[3] Badran, G., & Dhimish, M. (2023). Potential Induced Degradation in Photovoltaic Modules: A Review of the Latest Research and Developments. Solar, 3(2), 322-346. https://doi.org/10.3390/solar3020019

[4] Baradieh, K. I., Zainuri, M. A. A. M., Mohamed Kamari, N. A., Abdullah, H., Yusof, Y., Zulkifley, M. A., & Koondhar, M. A. (2024). A Study on the Impact of Different PV Model Parameters and Various DC Faults on the Characteristics and Performance of the Photovoltaic Arrays. Inventions, 9(5). https://doi.org/10.3390/inventions9050093

[5] Brahim, T., Abdelati, R., & Jemni, A. (2024). Dynamic simulation of roll bond PVT solar collector under Simulink/Matlab. Engineering Research Express, 6(4). https://doi.org/10.1088/2631-8695/ad8ff5

[6] Calcabrini, A., Procel Moya, P., Huang, B., Kambhampati, V., Manganiello, P., Muttillo, M., Zeman, M., & Isabella, O. (2022). Low-breakdown-voltage solar cells for shading-tolerant photovoltaic modules. Cell Reports Physical Science, 3(12). https://doi.org/10.1016/j.xcrp.2022.101155

[7] Datta, S., Baul, A., Sarker, G. C., Sadhu, P. K., & Hodges, D. R. (2023). A Comprehensive Review of the Application of Machine Learning in Fabrication and Implementation of Photovoltaic Systems. IEEE Access, 11, 77750-77778. https://doi.org/10.1109/access.2023.3298542

[8] Diniță, A., Rosca, C.-M., Stancu, A., & Popescu, C. (2025). Distributed IoT-Based Predictive Maintenance Framework for Solar Panels Using Cloud Machine Learning in Industry 4.0. Sustainability, 17(21). https://doi.org/10.3390/su17219412

[9] Elnozahy, A., Abd-Elbary, H., & Abo-Elyousr, F. K. (2024). Efficient energy harvesting from PV Panel with reinforced hydrophilic nano-materials for eco-buildings. Energy and Built Environment, 5(3), 393-403. https://doi.org/10.1016/j.enbenv.2022.12.001

[10] Iturralde Carrera, L. A., Alfonso-Francia, G., Constantino-Robles, C. D., Terven, J., Chávez-Urbiola, E. A., & Rodríguez-Reséndiz, J. (2025). Advances and Optimization Trends in Photovoltaic Systems: A Systematic Review. Ai, 6(9). https://doi.org/10.3390/ai6090225

[11] Iturralde Carrera, L. A., Garcia-Barajas, M. G., Constantino-Robles, C. D., Álvarez-Alvarado, J. M., Castillo-Alvarez, Y., & Rodríguez-Reséndiz, J. (2025). Efficiency and Sustainability in Solar Photovoltaic Systems: A Review of Key Factors and Innovative Technologies. Eng, 6(3). https://doi.org/10.3390/eng6030050

[12] Jacob, E., & Farzaneh, H. (2025, Apr 4). Modeling and performance evaluation of hybrid photovoltaic thermal, wind, and battery microgrids using optimization and dynamic simulation. Sci Rep, 15(1), 11528. https://doi.org/10.1038/s41598-025-95149-w

[13] Lazaroiu, A. C., Gmal Osman, M., Strejoiu, C.-V., & Lazaroiu, G. (2023). A Comprehensive Overview of Photovoltaic Technologies and Their Efficiency for Climate Neutrality. Sustainability, 15(23). https://doi.org/10.3390/su152316297

[14] Liu, S., Li, S., Yang, Q., & Lin, M. (2025). Synergistic optical and thermal management for solar water and electricity co-generation via a front-side coupling strategy. Cell Reports Physical Science, 6(8). https://doi.org/10.1016/j.xcrp.2025.102720

[15] Liu, X., Xia, H., Li, K., Lu, Y., Lv, S., Zhao, Q., Song, W., & Wang, L. (2024, Sep 18). The real-time shadow detection of the PV module by computer vision based on histogram matching and gamma transformation method. Sci Rep, 14(1), 21781. https://doi.org/10.1038/s41598-024-71710-x

[16] Mamodiya, U., Kishor, I., Garine, R., Ganguly, P., & Naik, N. (2025, May 19). Artificial intelligence based hybrid solar energy systems with smart materials and adaptive photovoltaics for sustainable power generation. Sci Rep, 15(1), 17370. https://doi.org/10.1038/s41598-025-01788-4

[17] Muthuvel Raj, S., & Pawan Kumar, V. (2024). State-of-Art Techniques for Photovoltaic (PV) Power Systems and their Impacts. International Journal of Advanced Research in Science, Communication and Technology, 381-389. https://doi.org/10.48175/ijarsct-19956

[18] Oproescu, M., Schiopu, A.-G., Calinescu, V. M., Iana, V.-G., Bizon, N., & Sallah, M. (2024). Influence of Supplementary Oxide Layer on Solar Cell Performance. Engineering, Technology & Applied Science Research, 14(2), 13274-13282. https://doi.org/10.48084/etasr.6879

[19] Oulefki, A., Himeur, Y., Trongtirakul, T., Amara, K., Agaian, S., Benbelkacem, S., Guerroudji, M. A., Zemmouri, M., Ferhat, S., Zenati, N., Atalla, S., & Mansoor, W. (2024, Mar 30). Detection and analysis of deteriorated areas in solar PV modules using unsupervised sensing algorithms and 3D augmented reality. Heliyon, 10(6), e27973. https://doi.org/10.1016/j.heliyon.2024.e27973

[20] Rajendran, G., Raute, R., & Caruana, C. (2025). A Comprehensive Review of Solar PV Integration with Smart-Grids: Challenges, Standards, and Grid Codes. Energies, 18(9). https://doi.org/10.3390/en18092221

[21] Ramasamy, K., Murugesan, C., & Thamilkolunthu, S. (2023). Enhancing the efficiency of polytetrafluoroethylene-modified silica hydrosols coated solar panels by using artificial neural network and response surface methodology. High Temperature Materials and Processes, 42(1). https://doi.org/10.1515/htmp-2022-0273

[22] Sadiq, M., & Garba Ibrahim, I. S. A. (2025). Solar Photovoltaic Technologies: A Critical Review of Technological Developments, Implementation Challenges, and Future Prospects. International Journal of Modeling and Applied Science Research. https://doi.org/10.70382/caijmasr.v8i9.031

[23] Shaker, L. M., Al-Amiery, A. A., Hanoon, M. M., Al-Azzawi, W. K., & Kadhum, A. A. H. (2024). Examining the influence of thermal effects on solar cells: a comprehensive review. Sustainable Energy Research, 11(1). https://doi.org/10.1186/s40807-024-00100-8

[24] Sharma, K. K., & Chandra, P. (2025). Selective response surface methodology for Anti Reflective Coated Nano-film filter thickness optimization in hybrid PVT system. Engineering Applications of Computational Fluid Mechanics, 19(1). https://doi.org/10.1080/19942060.2024.2443119

[25] Vedulla, G., Geetha, A., & Senthil, R. (2022). Review of Strategies to Mitigate Dust Deposition on Solar Photovoltaic Systems. Energies, 16(1). https://doi.org/10.3390/en16010109

[26] Vishnuprakash, B., Abhirup, D., Sraman, C., Amrita, R., & Srotoswini, S. (2025). Innovative Power Strategies for CubeSats: Enhancing Solar Energy Capture and Efficient Storage Solutions. Acceleron Aerospace Journal, 4(1), 786-816. https://doi.org/10.61359/11.2106-2501

[27] Yang, Z., & Xiao, Z. (2023). A Review of the Sustainable Development of Solar Photovoltaic Tracking System Technology. Energies, 16(23). https://doi.org/10.3390/en16237768